ARTICLE

Analysis of Downhole Asphaltene Gradients in Oil Reservoirs with a New Bimodal Asphaltene Distribution Function

Julian Y. Zuo,*,[†] Oliver C. Mullins,[‡] Denise Freed,[‡] Dan Zhang,[†] Chengli Dong,[§] and Huang Zeng[†]

[†]DBR Technology Center, Schlumberger, Edmonton, AB T6N 1M9, Canada

[‡]Schlumberger Doll Research, One Hampshire Street, Cambridge, Massachusetts 02139, United States

[§]NAO, Schlumberger, 1325 S. Dairy Ashford, Houston, Texas 77077, United States

ABSTRACT: Downhole fluid analysis (DFA) has been successfully used to describe reservoir connectivity and fluid properties. DFA not only measures bulk fluid properties such as the gas—oil ratio (GOR), density, and light-end compositions of CO_2, CH_4, C_2H_6, C_3H_8—C_5H_{12} fraction, and hexane and heavier (hexane +) fractions but also color (optical density) that is related to the heavy ends (asphaltenes and resins) in real time at downhole conditions. Therefore, color gradient analysis in oil columns becomes essential to determine reservoir complexities. In this paper, a new bimodal Γ-distribution function (asphaltene molecules + nanoaggregates and clusters) was proposed to characterize asphaltene components. A thermodynamic asphaltene-grading model was also developed to describe equilibrium distributions of heavy ends (heavy resins and asphaltenes) in oil columns using the multicomponent Flory—Huggins regular solution model coupled with a gravitational contribution. The variations of oil properties (such as molar volume, molar mass, solubility parameter, and density) with depth were calculated by the equation of state (EOS). The primary factors governing asphaltene distribution in reservoirs are the gravitational term, which is determined in part by the size of the asphaltene colloidal particle, and the solubility term, which is determined in large part by the GOR (composition). Consequently, it is critical to accurately measure both the fluid coloration and the GOR (composition) to understand the asphaltene gradient in oil columns. The results obtained in this work are in accordance with the Yen—Mullins model in asphaltene science. In particular, if asphaltenes are equilibrated in an oil reservoir, then a massive fluid flow through the reservoir had to have taken place, and permeable rocks are required, thereby implying connectivity, because asphaltenes necessarily enter the reservoir out of their ultimate equilibrium at the beginning of the reservoir charging. Therefore, a new powerful approach is established for conducting DFA color and GOR gradient analysis by coupling advanced asphaltene science with DFA technology (profiling of fluids) to address reservoir connectivity.

INTRODUCTION

Downhole fluid analysis (DFA) has been successfully used to delineate reservoir attributes such as vertical and lateral connectivity and properties of the produced fluids.[1–8] DFA not only measures bulk fluid properties such as the gas—oil ratio (GOR), density, and light-end compositions of CO_2, CH_4, C_2H_6, C_3H_8—C_5H_{12} fraction, and hexane and heavier (hexane +) fractions more accurately but also color (optical density, OD) that is linearly related to the heavy ends (asphaltenes and heavy resins) in real time at downhole conditions. In addition, the color measurement is one of the most robust measurements in DFA. Therefore, the analysis of color gradients, especially in conjunction with GOR (composition) gradients, in oil columns becomes vital to discerning reservoir complexities.

Asphaltenes are defined as the hydrocarbon fractions soluble in toluene and insoluble in n-heptane, which are heavy polycyclic aromatic compounds forming nanocolloidal particles dispersed and/or suspended in oil. These nanocolloidal aggregates are the heaviest components in crude oil with by far the lowest effective diffusion coefficients in the oil.[9] Gravitational segregation tends to push asphaltenes down in an oil column, whereas light hydrocarbons such as methane and other dissolved gases tend to rise in the column. In addition, because light hydrocarbons and high-GOR oils are poor solvents for asphaltenes, asphaltenes

are expelled from the high-GOR top of the oil column. That is, both gravity and solubility tend to make asphaltene composition low at the top of the oil column. The fluids necessarily enter the reservoir out of their ultimate equilibrium at the beginning of reservoir charging, so it requires considerable fluid flow and permeable rocks to establish fluid equilibrium in the reservoir. Thus, fluids that are determined to be in equilibrium in different regions of the reservoir suggest that those reservoir regions are connected. In particular, if asphaltenes are equilibrated in spite of their small transport coefficients, the connectivity is implied because flow barriers would greatly impede asphaltene equilibration in the reservoir. Any sealing barrier or flow restriction would interrupt the movement and migration of asphaltenes. In contrast the presence of a discontinuous asphaltene composition vertically or laterally within the reservoir explicitly indicates a boundary for fluid flow. Although asphaltene gradients do not explicitly prove reservoir connectivity, the lack of an asphaltene gradient indicates a lack of connectivity. The recent advances in asphaltene science from the laboratory and field data have

demonstrated that asphaltenes are dispersed and/or suspended in crude oils and/or solvents in three forms: molecules, nano-aggregates, and clusters of nanoaggregates.[8−15] This provides us with a new foundation for methods of determining flow connectivity in the reservoir. In particular, in situ measurements of color (thus asphaltene content) and GOR (composition) by DFA in the reservoir enable coupling data with new thermodynamic models to determine the state of the asphaltene distribution. This distribution can often be used to assess reservoir connectivity. Therefore, a thermodynamic model is required to analyze DFA color and GOR (compositional) grading data.

Cubic equations of state (EOS's) have been broadly and successfully used to simulate reservoir fluid properties such as GOR and gas-retrograde dew-condensate phase transitions.[16−22] However, the previous cubic EOS's have not been able to handle asphaltenes accurately, in part because there were no appropriate ways of characterizing asphaltenes accurately. Because asphaltene properties, such as the critical properties and acentric factors required in the EOS calculations, cannot be measured experimentally due to decomposition prior to reaching their critical temperature, they were empirically assigned and/or extrapolated from light-hydrocarbons using property correlations. Moreover, the molecular and colloidal structures of asphaltenes are unknown, and even the order of magnitude of asphaltene molecular weight has been debated for many years.[10] Without knowing asphaltene size, the gravity term could not be assessed. Consequently, the EOS approach has been successfully used to calculate compositional gradients with depth for reservoir fluids without the incorporation of asphaltenes.[23−28] Indeed, corresponding workflows of light ends (CO_2, CH_4, C_2H_6, C_3H_8–C_5H_{12}, and hexane +) have been used to determine compartmentalization and/or nonequilibrium distributions of reservoir fluids particularly for significant compositional gradients with depth by Zuo et al.[28] If formation conditions are far away from the critical points of the reservoir fluids, the compositional gradients if equilibrated are usually not significant, and thus analysis of the light ends cannot be used for analyzing reservoir connectivity. However, color (asphaltene) gradients are usually found to be considerable in the reservoir because of gravity and the variation of the live oil (fluid that contains substantial amount of dissolved gas) solubility parameter. Therefore, the color (asphaltene) gradients with depth can be employed to analyze reservoir compartmentalization or connectivity.

Although cubic EOS's can be employed to describe asphaltene distributions in oil columns as described by Zuo et al.,[29,30] it makes calculations a bit complicated because of the large molar mass of asphaltene nanoaggregates and clusters. These large asphaltene nanoaggregates and clusters affect the calculations of conventional fluid properties and phase behavior significantly because a conventional cubic EOS is unsuitable for such complicated systems, especially for the fluids with a relatively high asphaltene composition. The perturbed-chain statistical associating fluid theory (PC-SAFT) EOS has been applied to asphaltene precipitation in flow assurance.[31−34] However, there still exist uncertainties in the characterization of asphaltenes at downhole conditions. On the other hand, the Flory–Huggins regular solution model has been widely and successfully employed to model asphaltene precipitation issues.[35−39] Nevertheless, the PC-SAFT EOS and the Flory–Huggins type of solubility model have not been extended to model asphaltene distributions in oil columns. Although Hirschberg[40] suggested the use of the regular solution model to describe asphaltene gradients, asphaltene dispersions in

crude oil were not fully understood at that time, nor was there a thorough understanding of the solubility of asphaltenes in crude oils. Therefore, a new approach is needed to describe asphaltene distributions in oil columns by combining the Flory–Huggins regular solution model with the gravitational contribution, that is, an EOS + Flory–Huggins regular solution model approach.

To achieve this purpose, a new thermodynamic approach was developed for analyzing asphaltene gradients in oil columns. This approach consists of two parts: the EOS and the Flory–Huggins regular solution model. In the first part, the EOS was applied to calculate compositional and property gradients without taking asphaltenes into consideration in particular. The variations of bulk fluid properties such as density, molar volume, molar mass, and solubility parameter with depth were calculated by the EOS whose parameters were adjusted to match compositional and property gradients data measured by DFA or in laboratories. In the second part, a presumed two-group-multicomponent system was accounted for by the Flory–Huggins regular solution model: a solvent group of the oil mixture without asphaltenes and a solute group of the asphaltenes in the oil mixture. Furthermore, asphaltenes were treated as multiple asphaltene subfractions (pseudocomponents) using a new bimodal Γ-distribution function. The asphaltene properties were estimated by the use of the empirical correlations taken from the open literature. The average molar mass of asphaltene molecules, nanoaggregates, or clusters was determined by matching color gradient data measured by DFA and compared with recent advances in asphaltene science (the Yen–Mullins model[10]). A few field case studies were used to validate the thermodynamic method, and the obtained results indicate that the developed method can be successfully used to delineate fluid complexities and reservoir architecture.

■ DOWNHOLE FLUID ANALYSIS AND EOS BASED DATA INTERPRETATION

The first generation of DFA tools was primarily for real time monitoring of oil-based mud (OBM) filtrate contamination during downhole fluid sampling as well as to distinguish hydrocarbon and water fractions in the 1990s. The second generation of DFA tools was introduced in the early 2000s with the capability of measuring hydrocarbon composition (CH_4, C_2H_6–C_5H_{12}, and hexane +), GOR, and fluorescence properties at downhole conditions. The third generation of DFA tools was introduced recently.[3] The new DFA tool integrates multiple sensors in a single platform and provides significantly more accurate and complete fluid properties than previous fluid analyzers. It incorporates an absorption spectrometer, a fluorescence sensor, density measurement, resistivity, and pressure/temperature sensors, which provides real time in situ fluid GOR, compositions (CH_4, C_2H_6, C_3H_8–C_5H_{12}, and hexane +), CO_2 content, fluid density, water pH, fluorescence/reflection intensities and resistivity, and OBM filtrate contamination level (volume of OBM filtrate in contaminated oil divided by volume of contaminated oil). Compared to the previous DFA tools, not only a new density measurement at downhole conditions is added, but also the accuracy of all of the fluid property measurements is substantially enhanced through newly designed hardware and fundamentally improved interpretation algorithms.

The DFA technique utilizes the optical spectroscopy spectrum of crude oils, gases, OBM filtrates, and water in the visible and near-infrared (NIR) wavelength regions. The optical density (OD)
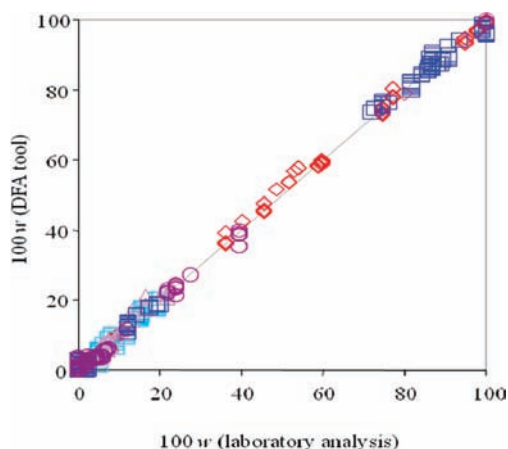
Figure 1. Evaluation of fluid property measurements of the new generation DFA tool on composition. $\diamond$, CH_4; light blue $\square$, C_2H_6; $\triangle$, C_3H_8–C_5H_{12} fraction; dark blue $\square$, C_6H_{14} + fraction; $\bigcirc$, CO_2. The mass fractions w measured by DFA are in good agreement with the laboratory measurements.

Figure 2. Evaluation of fluid property measurements of the new generation DFA tool on GOR. The GORs measured by DFA are in good agreement with the laboratory measurements.

is defined as the logarithm of the intensity ratio of the incident light to the light transmitted through the fluid. The absorption difference between crude oil and OBM filtrate at the low wavelength region (< 1000 m) provides a physical basis for monitoring and quantitatively determining OBM contamination during the sampling process. The two distinguished absorption peaks of water at (1450 to 2000) nm are used to quantitatively determine the water fraction in the flowline of fluid analyzer. The composition analysis uses absorption properties of hydrocarbon components in the NIR region. Methane, ethane, and propane have different absorption peaks in both wavelength and magnitude. From combination principle, hydrocarbon composition is derived in groups of methane, ethane, propane to pentane, and hexane and heavier hydrocarbons. Fluid GOR is then determined from the composition. The detailed methods are described by Mullins.[52]

The new DFA tool was tested extensively at all development stages. A series of laboratory experiments were designed to test and qualify individual sensors as well as the actual DFA tools. In the tests, a research grade laboratory spectrometer and other PVT laboratory equipments were used along with the DFA tool, and test fluids included actual crude oils, condensate and dry gases, pure compounds, standard viscosity fluids, and even drilling mud for cleanup efficiency check. The new DFA has also gone through extensive field tests at various conditions and with all types of formation fluids. Measurement accuracy, reliability, and an interpretation algorithm of the new DFA tool were thoroughly evaluated through laboratory and field tests.[3,18] Figures 1 and 2 compare the DFA measurements with laboratory data for compositions and GOR. The compositions and GOR measured by DFA tools and in laboratories are in good agreement. The results show that the new DFA tools provide good fluid property measurements across a wild range of fluids at downhole conditions.[3,18] For the readers who are not familiar with oil and gas, some basic terms are given in the Appendix.

Zuo et al.[18] developed a new approach to maximize the value of DFA data, perform quality assurance and/or quality control of DFA data, and establish a fluid model (EOS) for DFA predi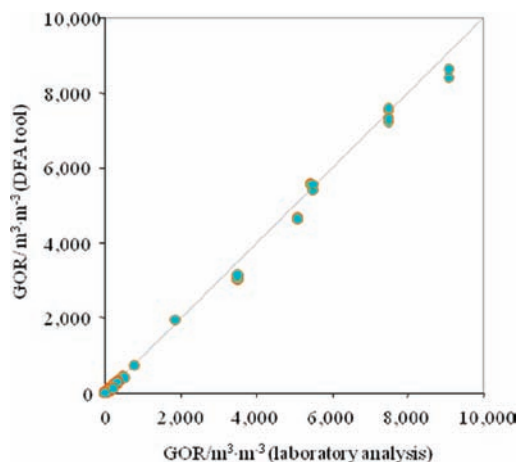ctions. The basic inputs from DFA measurements are mass percentages of CO_2, CH_4, C_2H_6, C_3H_8–C_5H_{12}, and hexane + and fluid density. A new method was proposed to delump and characterize the DFA measurements of C_3H_8–C_5H_{12} and hexane + into full-length compositional data. C_3H_8–C_5H_{12} is delumped into propane, butane, and pentane fractions by means of the component ratio correlations developed based on a large database consisting of different fluids all over the world.[18] Hexane + is characterized and extrapolated to single carbon number fractions (such as hexane, heptane, octane, etc.) by assuming that the relation between mass fractions and molar masses (or carbon numbers) follow an exponential distribution, which is widely used in natural existing oil and gas systems.[18,19] The full-length compositional data predicted by the new method were compared with the laboratory-measured gas chromatography (GC) data up to C_{30+} for more than 1000 different types of reservoir fluids. These fluids have GOR = (1.4 to 25 000) $m^3 \cdot m^{-3}$ and API gravity = (9 to 50). Figure 3 shows a typical comparison of delumped compositions with laboratory GC data for gas condensate, black oil, and heavy oil. A good agreement was achieved between the delumped and the GC compositions.[18] In addition, on the basis of the delumped and characterized full-length compositional data, an EOS model was established that could be applied to predict fluid phase behavior and physical properties by virtue of DFA data as inputs. The EOS predictions were validated and compared with the laboratory-measured fluid properties for more than 1000 different types of reservoir fluids. The GOR, formation volume factor (volume of oil with dissolved gas at high pressure divided by volume of stock tank oil (STO) at standard conditions $T = 288.7$ K and $p = 0.1$ MPa), and density predictions were in good agreement with the laboratory measurements.[18] The deviations of the predicted GOR, formation volume factor, and density are 4.8 %, 1.5 %, and 1.1 %, respectively. The established EOS model was then able to predict other fluid properties, and the results were in good agreement with the laboratory measurements as well.

Consequently, the EOS model proposed laid a solid foundation for DFA log predictions (compositional and property gradients with depth), which have successfully been integrated with DFA measurements in real time to delineate compositional and property gradients in oil columns.[28–30] The EOS model is also used to calculate variations of bulk fluid properties.
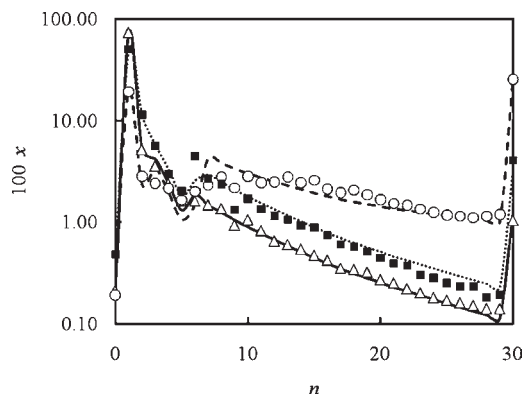
Figure 3. Comparison of delumped and laboratory-measured mole fraction x for three typical fluids. Carbon number $n = 0$ means CO_2; carbon number $n = 30$ means C_{30+}; $\triangle$, laboratory composition for gas condensate; —, delumped composition for gas condensate; ■, laboratory composition for black oil; ···, delumped composition for black oil; ○, laboratory composition for heavy oil; ---, delumped composition for heavy oil. The delumped compositions are in good agreement with the laboratory measurements.

■ THE FLORY—HUGGINS REGULAR SOLUTION MODEL FOR ASPHALTENE GRADIENTS IN OIL COLUMNS

It is assumed that a reservoir fluid is treated as a mixture with two groups of multicomponents: a solvent group (nonasphaltene components or maltene) and a solute group. Asphaltenes are divided into a different number of subfractions using a bimodal Γ-distribution function which is described later. The mixture (bulk fluid—whole oil) properties are represented by no subscripts in the following derivation, and they are calculated by the EOS described in the previous section and relevant references.[17,18,28−30]

To calculate compositional gradients with depth in a reservoir column, it is usually assumed that all components have zero mass flux defining a steady state for a mixture with N-components. The equation for component i is given by Zuo et al.[28,29]

$$(d\mu_i)_T + M_i g dh + F_{Ti} d \ln T = 0 \qquad i = 1, 2, ..., N \quad (1)$$

where μ_i, M_i, g, and T stand for the chemical potential and molar mass of component i, gravitational acceleration, and absolute temperature, respectively. The term $(d\mu_i)_T$ denotes the chemical potential change of component i in a small interval (dh) of depth at isothermal conditions. F_{Ti} is the thermal diffusion flux of component i, which takes into account temperature gradients in the oil column. If it is assumed that the reservoir is isothermal, the thermal diffusion term in eq 1 vanishes. In some treatments, the gravity term is incorporated into the chemical potential term,[41] but the results are the same.

In the EOS approach, the chemical potential μ_i can be calculated in terms of the fugacity f_i of component i. Hence, eq 1 can be expressed as

$$RTd \ln f_i + M_i g dh + F_{Ti} d \ln T = 0 \qquad i = 1, 2, ..., N \quad (2)$$

This formula is widely used to calculate compositional gradients with depth for reservoir fluids by virtue of cubic EOS.[23−29]

According to the thermodynamic relation,[42] the isothermal chemical potential change of component i is a function of pressure (p) and component mole fractions (x):

$$(d\mu_i)_T = \left(\frac{\partial \mu_i}{\partial p}\right)_{T,x} dp + (d\mu_i)_{T,p} = \overline{V}_i dp + (d\mu_i)_{T,p} \quad (3)$$

where the term $(d\mu_i)_{T,p}$ is the chemical potential change of component i in a small interval of depth at constant temperature and pressure. Substituting eq 3 and an equilibrium hydraulic equation ($dp = \rho g dh$) into eq 1 and assuming that the reservoir is isothermal, we obtain

$$(d\mu_i)_{T,p} = (\rho \overline{V}_i - M_i)g dh = \overline{V}_i \left(\rho - \frac{M_i}{\overline{V}_i}\right)g dh \quad (4)$$

It is further assumed that the partial molar volume of component $i V_i$ is equal to its molar volume $V_{m,i}$, which is reasonable for highly incompressible components such as asphaltenes. Therefore, $\rho_i = (M_i/V_{m,i})$ is the density of component i. Thus, eq 4 can be rewritten for asphaltene components as

$$(d\mu_{a_i})_{T,P} = V_{m,a_i}(\rho - \rho_{a_i})g dh \quad (5)$$

where subscript a_i is the ith subfraction of asphaltenes. $(d\mu_{a_i})_{T,P}$, ρ_{a_i}, and V_{m,a_i} are the chemical potential change at constant temperature and pressure, density, and molar volume of the ith subfraction of asphaltenes, respectively. ρ is the density of the bulk fluid. The chemical potential change of asphaltene components at constant temperature and pressure can be estimated by the multicomponent Flory—Huggins regular solution model[35−37,42]

$$\frac{(d\mu_{a_i})_{T,p}}{RT} = d\left[\ln \phi_{a_i} + \left(1 - \frac{V_{m,a_i}}{V_m}\right) + \frac{V_{m,a_i}}{RT}(\delta_{a_i} - \delta)^2\right] \quad (6)$$

where R is the universal gas constant. ϕ_{a_i}, δ_{a_i}, and V_{m,a_i} stand for the volume fraction, solubility parameter, and molar volume of the ith subfraction of asphaltenes. V_m and δ are the molar volume and solubility parameter of the bulk fluid. The first two terms on the right-hand side of eq 6 stand for the chemical potential contribution from the combinatorial entropy change of mixing which is estimated by the Flory—Huggins polymer-like contribution.[42] The third term arises from the enthalpy change upon mixing computed by means of the regular solution model.[42]

Substituting eq 6 into eq 5, integrating it at two depths (h_2 and h_1), if $\Delta h = h_2 - h_1$ is small enough, and we ignore the density difference between h_2 and h_1, we have

$$\frac{\phi_{a_i}(h_2)}{\phi_{a_i}(h_1)} = \exp\left\{\left[\left(\frac{V_{m,a_i}}{V_m} - 1\right)\right]_{h_2} - \left[\left(\frac{V_{m,a_i}}{V_m} - 1\right)\right]_{h_1}\right.$$
$$+ \left[\frac{V_{m,a_i}}{RT}(\delta_{a_i} - \delta)^2\right]_{h_1} - \left[\frac{V_{m,a_i}}{RT}(\delta_{a_i} - \delta)^2\right]_{h_2}$$
$$\left. + \frac{V_{m,a_i}g(\rho - \rho_{a_i})(h_2 - h_1)}{RT}\right\} \quad (7)$$

Therefore, the volume fraction variations of asphaltenes with depth depend on three terms: the entropy, solubility (enthalpy), and gravitational contributions. The solubility and gravitational terms enhance the asphaltene gradient, whereas the entropy term reduces the asphaltene gradient. In particular, if an oil column has a large GOR (compositional) gradient, then the solubility term can dominate, in large part because of the nonexistent solubility of asphaltenes in gas (mainly consisting of methane). In contrast, if the GOR (compositional) gradient is very small, such as in the case of a highly undersaturated low-GOR (GOR < 150 m³·m⁻³) black oil, then the gravity term dominates asphaltene distributions in the oil column. Consequently, to understand asphaltene gradients, it is crucial to measure both the asphaltene (coloration) and GOR (composition) gradients in the column.
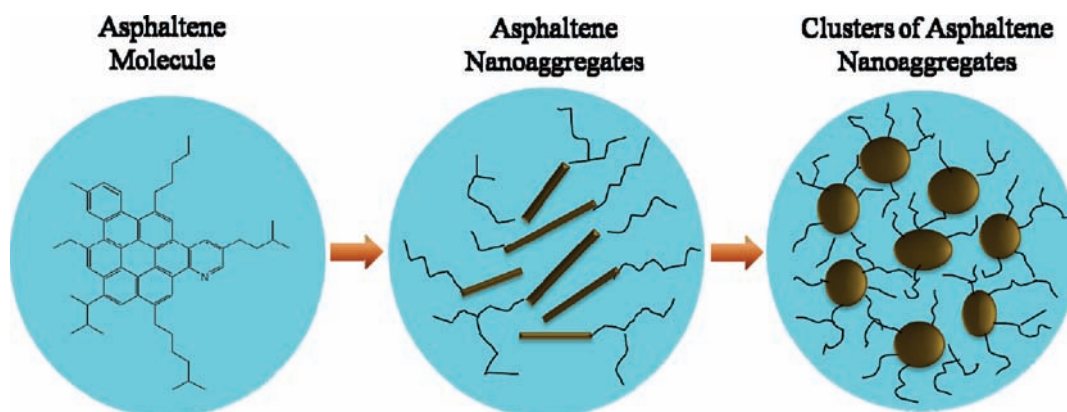
Figure 4. Yen−Mullins model, the new first principle paradigm of asphaltenes.[10] Asphaltene molecules have average molar mass of $\approx$ 750 g·mol^{-1}. Nanoaggregates have $\approx$ 6 molecules, and clusters have $\approx$ 8 nanoaggregates. Condensates have a molecular dispersion of heavy ends, stable black oils have asphaltenes in nanoaggregates, and unstable black oils and heavy oils have at least some asphaltenes in clusters of nanoaggregates.

■ BIMODAL ASPHALTENE MOLAR MASS DISTRIBUTIONS AND ASPHALTENE CHARACTERIZATION

In recent years, considerable progress has been made in virtually all areas of asphaltene science.[9] In particular, the molecular and colloidal structure of asphaltenes has largely been resolved and is now codified in the Yen−Mullins model.[10] The Yen−Mullins model provides us with a framework/foundation for understanding the dispersion of asphaltenes in crude oil and has found application and success in oilfield case studies.[10]

In the Yen−Mullins model, asphaltenes are dispersed and/or suspended in crude oils and/or in solvents in three forms: molecules, nanoaggregates, and clusters of nanoaggregates, as depicted in Figure 4.

Asphaltene molecules have an average molar mass of $\approx$ 750 g·mol^{-1} in a range of (400 to 1000) g·mol^{-1}. The number of fused aromatic rings (FAR) per asphaltene polycyclic aromatic hydrocarbon (PAH) is $\approx$ 7. The critical nanoaggregate concentration of asphaltenes (CNAC) is (50 to 150) mg·L^{-1}, aggregation number of nanoaggregates $\approx$ 6, and the concentration of asphaltene cluster formation (2 to 5) g·L^{-1}, and the clusters have $\approx$ 8 nanoaggregates.[43,44] Laboratory and field data have proven the Yen−Mullins model. Asphaltene molecules are dissolved in condensate (e.g., GOR > $\approx$ 356 m^3·m^{-3}); nanoaggregates are dispersed in stable black oil (e.g., $\approx$ 20 m^3·m^{-3} < GOR < $\approx$ 356 m^3·m^{-3}), and some clusters are at least stably suspended in heavy oil (e.g., GOR < $\approx$ 20 m^3·m^{-3}) and asphaltene-destabilized black oil. Coupling this advanced asphaltene science with the new generation of DFA technology provides us with a new and powerful approach for delineating reservoir connectivity through asphaltene gradient analysis.

If reservoir fluids contain a large fraction of asphaltenes and/or asphaltenes are unstable under reservoir conditions, then not only do the common asphaltene nanoaggregates with about 2 nm in spherical diameter exist, but also clusters of asphaltene nanoaggregates ($\approx$ 5 nm) are stably suspended in reservoir fluids. Therefore, a new bimodal asphaltene molar mass distribution function is proposed to describe asphaltene components. The new asphaltene bimodal probability density function is expressed as

$$p(M) = \sum_{k=1}^{k=2} z_k p_k(M) \tag{8}$$

where z_k and $p_k(M)$ are the fraction and probability density function of the common asphaltene nanoaggregates including molecules, as well as those of the clusters of asphaltene nanoaggregates, respectively, subjecting to $\sum z_k = 1$.

The three-parameter Γ function is chosen for describing the molar mass distribution of asphaltene nanoaggregates and clusters.[45,46] The probability density function is given by

$$p_k(M) = \frac{(M - M_{k,\min})^{\alpha-1} \exp[-(M - M_{k,\min})/\beta]}{\beta^\alpha \Gamma(\alpha)} \tag{9}$$

where α, β, and $M_{k,\min}$ are the three parameters defining the distribution. $M_{1,\min}$ can be set to the number of $\approx$ 500 g·mol^{-1} for asphaltene nanoaggregates including asphaltene molecules since it represents the minimum molar mass to be included in asphaltene nanoaggregates.[10] $M_{2,\min}$ can be set to $\approx$ 3000 g·mol^{-1} for the clusters of asphaltene nanoaggregates as it stands for the minimum molar mass to be included in asphaltene clusters.[10] If α is given, β can be estimated by

$$\beta = \frac{(M_{k,\text{avg}} - M_{k,\min})}{\alpha} \tag{10}$$

The parameter α can be determined by fitting experimental data of asphaltene molar mass distributions. For asphaltenes and bitumens, Tharanivasan et al.[37] found α = 3.5. This value is also used in this paper. Therefore, the undetermined parameter is the average molar mass of asphaltene molecules, nanoaggregates, and/or clusters, which can be treated as an adjustable parameter to match DFA color (OD) gradient data in the reservoir. In this manner, a distribution of asphaltenes (or colored heavy resins) dispersed/suspended in crude oils as molecules, nanoaggregates, and clusters can be accounted for. If there are only asphaltene molecules (e.g., colored asphaltene-like heavy resins in condensates), the average molar mass of asphaltene molecules is about 750 g·mol^{-1}. If there are no asphaltene clusters but nanoaggregates, then the average molar mass of asphaltene nanoaggregates is about 3000 g·mol^{-1} with about 2 nm in spherical diameter. If there are asphaltene clusters only, then the average molar mass of asphaltene clusters is about 25 000 g·mol^{-1} with about 4 nm in spherical diameter. In these cases, only one term is used in eq 8. If asphaltene nanoaggregates and clusters coexist, then $M_{1,\text{avg}}$ and

$M_{2,\text{avg}}$ are set to (≈ 3000 and $\approx 25\,000$) g·mol^{-1}, respectively. Then z_1 is adjusted to match the DFA data in oil columns.

The Gaussian quadrature method is used to discretize the continuous Γ-distribution, $p_k(M)$, using N quadrature points.[46] It is noted that the calculated results are similar when $N \geq 3$. In this work, therefore, $N = 5$ is used; that is, five pseudocomponents/subfractions represent asphaltene nanoaggregates including molecules, and the other five pseudocomponents/subfractions stand for asphaltene clusters.

■ DETERMINATION OF THE PARAMETERS REQUIRED IN CALCULATIONS

After characterizing asphaltenes, the asphaltene properties required in the calculations can be computed by the following correlations taken from the open literature.

It is assumed that the properties of the asphaltene are independent of depth and the reservoir fluid remains a single phase or stable molecular or colloidal dispersion at all depths. The density of asphaltene subfraction i in kg·m^{-3} is calculated by the expression[36]

$$\rho_{a_i} = 670 M_{a_i}^{0.0639} \qquad (11)$$

where M_{a_i} is the molar mass of asphaltene subfraction i obtained via discretizing the Γ-distribution function. The solubility parameter of asphaltene subfraction i in MPa$^{0.5}$ is estimated by the expression of Alboudwarej et al.[36]

$$\delta_{a_i} = \sqrt{A\rho_{a_i}} \qquad (12)$$

where $A = 0.366$ kJ·g^{-1}. For instance, $\delta_{a_i} = 20.957$ MPa$^{0.5}$ if $\rho_{a_i} = 1200$ kg·m^{-3}. The temperature dependence of asphaltene solubility parameters is taken into account by the following relation[39]

$$\delta_{a_i}(T) = \delta_{a_i}(T_0)[1 - 1.07 \cdot 10^{-3}(T - T_0)] \qquad (13)$$

where T_0 is the reference temperature for solubility parameters of asphaltenes. The values computed by eq 12 were assumed to be those at $T_0 = 298.15$ K (typical room temperature). For instance, if it is assumed that the molar mass of asphaltene molecules is 750 g·mol^{-1}, then $\rho_a = 1.023$ g·cm^{-3} computed by eq 11, δ_a ($T_0 = 298$ K) = 19.35 MPa$^{0.5}$ estimated by eq 12, and $\delta_a(T = 398$ K) = 17.28 MPa$^{0.5}$ calculated by eq 13. It can be seen that an increase of 100 K in temperature causes a decrease in the asphaltene solubility parameter by ≈ 11 %. The influence of pressure on solubility parameters of asphaltenes is ignored because of the incompressibility of the asphaltenes.

The compositional and fluid property gradients (fluid profile) proposed by the method of Zuo et al. (described in the previous sections)[17,18,28−30] are computed for bulk oil by solving eq 2 using the Peng−Robinson EOS[47,48] with the Peneloux volume translation.[49] The EOS parameters are adjusted to match phase behavior and compositional gradient data measured by DFA and/or in laboratories. The solubility parameter of the bulk oil is computed using the established EOS as well. That is, the reservoir fluid is treated as a whole. Then its internal energy (Δu) and molar volume (v) are calculated by the EOS, and the solubility parameter is computed by the definition $\delta = (\Delta u/v)^{0.5}$. Recently, Zuo et al.[50] developed a simple relation to estimate the solubility parameter of live fluids based on live fluid densities, which can also be used for the solubility parameter of bulk fluids. In this way, the solubility parameter of bulk fluids can easily be determined based on measured bulk fluid density.
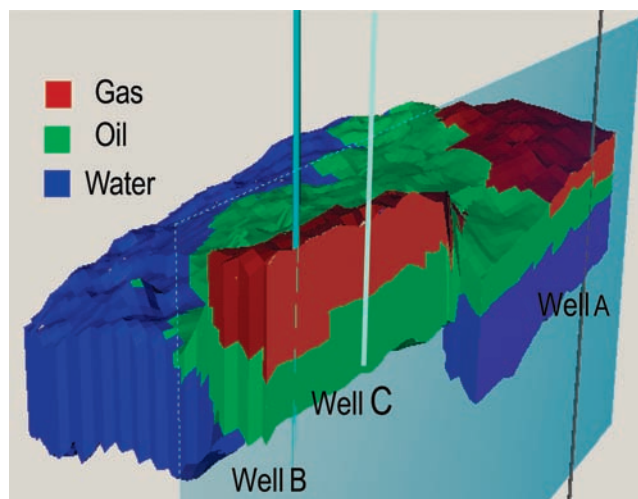

Figure 5. Norway reservoir with two gas caps. The two gas/oil contacts (GOC) differ by 18 m true vertical depth. Either there is a lateral nonequilibrium or compartmentalization.

In the thermodynamic model mentioned above, the only undetermined parameter is the average molar mass of asphaltene molecules, nanoaggregates, or clusters, which is determined by matching the color gradient data measured by DFA. Therefore, it is critical to measure both the asphaltene (coloration) and GOR (composition) gradients in oil columns to conduct DFA asphaltene profiling. It should be noted that the fitting parameter must be consistent with values from the Yen−Mullins model in asphaltene science. Otherwise, the fitting process does not make any scientific sense, and the results are meaningless.

■ RESULTS AND DISCUSSIONS: FIELD CASE STUDIES

Case 1: Asphaltene-Like Heavy Resins in Condensate. Condensates have a very small number of asphaltenes because a large amount of dissolved gas and light hydrocarbons make them very poor solvents for asphaltenes. In addition, mechanisms of forming condensate reservoirs do not tend to generate asphaltenes. Therefore, there is very little crude oil color as determined by DFA in the near-infrared region. Nevertheless, there are asphaltene-like molecules, the heavy resins, which absorb visible light and even some in the near-infrared region. On the other hand, condensates have substantial GOR gradients with depth. Because condensates are compressible (large compressibility), the hydrostatic head pressure of the condensate column produces a density gradient in the column. The density gradient creates the driving force to create a chemical composition gradient. The lower density components tend to rise in the column, while the higher density components tend to settle in the column. This GOR gradient gives rise to a large solubility contrast for the heavy resins, thereby producing significant DFA color gradients. These gradients are useful to check for reservoir connectivity.

In the Norway case,[6] the condensate reservoir has large GOR (composition) gradients and two separate gas caps as shown in Figure 5. Both separate gas caps are thought to share a common oil leg. However, the two gas/oil contacts (GOCs) differ by 18 m true vertical depth (TVD). If the oil sand is continuous, then the reservoir fluid cannot be in equilibrium because there cannot be two different saturation pressures at one depth. The unexpected 18 m TVD difference of GOCs could be explained by two
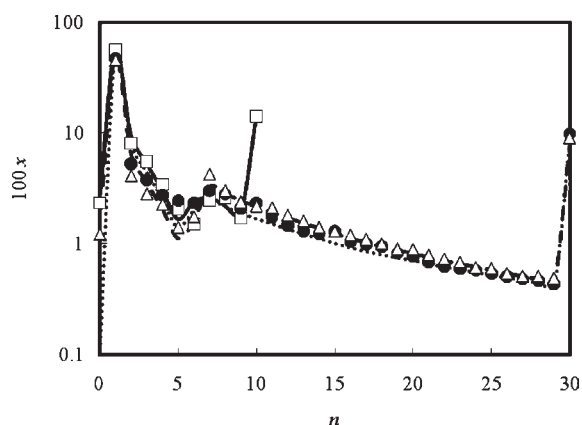
Figure 6. Comparison of delumped and laboratory-measured mole fraction x for the three fluids studied in this work. Carbon number $n = 0$ means CO_2; carbon number $n = 30$ means C_{30+}; □, laboratory composition for the fluid in case 1 (condensate analyzed up to C_{10+}); —, delumped composition for the fluid in case 1; △, laboratory composition for the fluid in case 2 (stable black oil); ···, delumped composition for the fluid in case 2; ●, laboratory composition for the fluid in case 3 (destabilized black oil); ---, delumped composition for the fluid in case 3. The delumped compositions are in good agreement with the laboratory measurements.

Figure 7. Phase envelope of the Norway reservoir fluid at the GOC in Well A. The formation pressure is equal to the bubble-point pressure at the GOC. The formation condition is not far away from the critical point. Large fluid compositional and property gradients are anticipated. ○, experimental bubble point; □, critical point calculated by EOS; —, bubble points calculated by EOS; ---, dew points calculated by EOS.
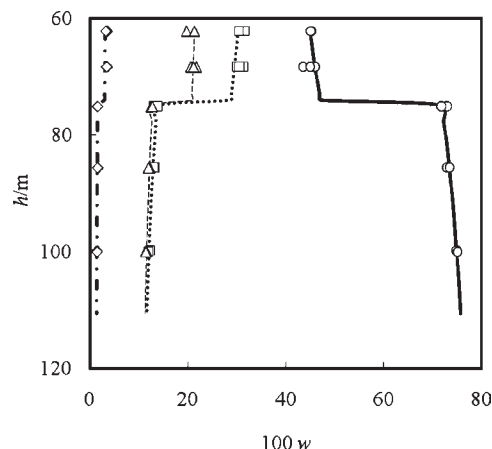
Figure 8. Comparison of the predicted and measured variations of mass fraction w with relative depth h for the Norway fluids in Well A. The compositions significantly change at the GOC, and the compositional gradients are large. The predictions are in good agreement with the measurements. ◇, CO_2 measured by laboratory; △, C_2–C_5 measured by laboratory; □, C_1 measured by laboratory; ○, C_{6+} measured by laboratory; ·-·, CO_2 calculated by EOS; ---, C_2 to C_5 calculated by EOS; ····, C_1 calculated by EOS; —, C_{6+} calculated by EOS.

reservoir descriptions: either the reservoir is compartmentalized, or there is a single compartment with a small lateral nonequilibrium.

The delumped compositions are compared with the laboratory measurements in Figure 6 for the three fluids studied in this work. The delumped compositions are in good agreement with the measured data. The fluid in case 1 was analyzed to C_{10+} in the laboratory (open squares). The EOS model was established by the method of Zuo et al.[18] The fluid properties were also matched by tuning the EOS model. The phase envelope is shown in Figure 7 for the fluid at the GOC in Well A. It can be seen that the fluid is a volatile condensate oil and the formation pressure is equal to the bubble pressure at the GOC (not far from its critical point). This fluid should exhibit significant compositional gradients according to Høier and Whitson.[23] Indeed, the data measured by DFA and laboratory and the EOS predictions have proved the large compositional gradients in this reservoir.

Figure 8 illustrates a comparison of the predicted compositions with the laboratory data (which are similar to DFA data) at the GOC in Well A. The compositions significantly change at the GOC, and the compositional gradients are large in the reservoir. The predictions are in good agreement with the laboratory-measured data.

Figure 9 compares the predicted GOR and live fluid density using the EOS with the laboratory-measured data, which are in good agreement. The EOS slightly underpredicts GOR and oil density in the oil zone. The GOR varies from (340 to 280) $m^3 \cdot m^{-3}$ in the oil column.

For simplicity, it was assumed that colored components of fluids are a mixture of colored asphaltene-like heavy resins, which was later proved to be consistent with the Yen–Mullins model, with the color proportional to the mass fraction of the colored resins. The three-parameter Γ-distribution function mentioned above was used to describe the molar mass distribution of the colored asphaltene-like resins at the reference point. The average molar mass was treated as an adjustable parameter by fitting the DFA-measured coloration gradient data in Well A. The fitting
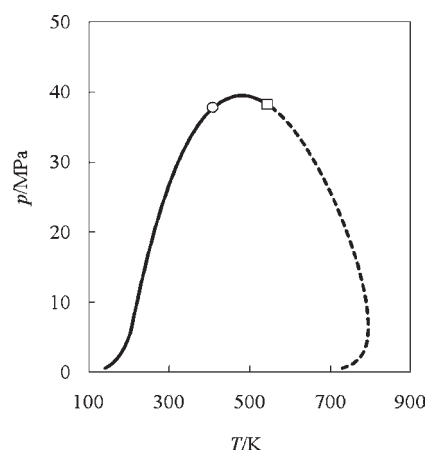
results are shown in Figure 10 with the adjusted average molar mass of 680 $g \cdot mol^{-1}$ for the colored asphaltene-like resins at a relative depth of about 63 m for Well A. The corresponding average density and molar volume are 1.017 $g \cdot cm^{-3}$ and 668.6 $cm^3 \cdot mol^{-1}$, respectively.

The color data (OD at 647 nm) from Well A follow a consistent trend predicted by the Flory–Huggins regular solution model except for the deepest point, which has a bit more color than anticipated and is near the oil–water contact (OWC). The color data from Well B (only available at two depths) are plotted on the same trend line at the top of the reservoir, but the deepest point, which is also near the OWC, is above the curve. This follows the trend from Well A, where fluids in the lower part of the reservoir have more color. The color data from the third well, referred to as Well C, are also on the same trend curve calculated
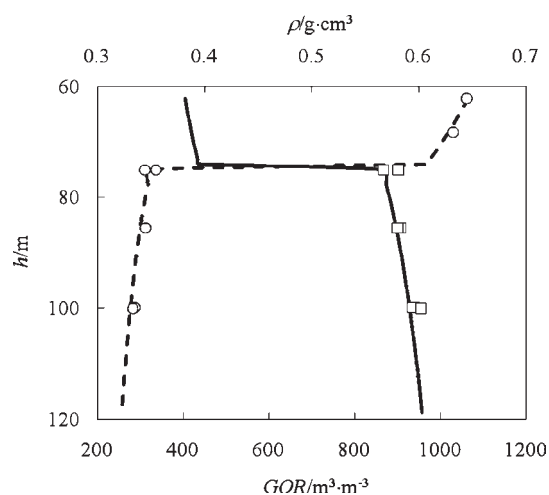
Figure 9. Comparison of the predicted and measured GOR and live fluid density ρ variations with relative depth h for the Norway fluids in Well A. The EOS predictions are in accord with the laboratory measurements. $\bigcirc$, GOR measured by laboratory; $\square$, live fluid density measured by laboratory; ---, GOR calculated by EOS; —, live fluid density calculated by EOS.

Figure 10. Variations of OD (color) with relative depth h for the Norway fluids for Wells A, B, and C. The theoretical fit is consistent with a molecular distribution of asphaltene-like resin molecules. The large (four times) gradient of color in 40 m is due to the large GOR gradient; the solubility term dominates the color variation, whereas the gravity term contributes little. $\diamond$, Well A measured by CFA (composition fluid analyzer); $\blacksquare$, Well A measured by LFA (live fluid analyzer); $\square$, Well B measured by CFA; $\bullet$, Well B measured by LFA; $\bigcirc$, Well C measured by CFA; $\triangle$, Well C measured by LFA; —, calculation by the asphaltene-grading model with an average asphaltene molar mass of 680 g·mol^{-1} at the reference depth; · · ·, calculation by the asphaltene-grading model with an average asphaltene molar mass of 680 g·mol^{-1} at the reference depth and C_1 and C_{6+} composition (weight percent) deviations by 0.5 and 3, respectively.

by the Flory–Huggins regular solution model. This is consistent with reservoir connectivity. The subsequent production data have proven the connectivity of the reservoir. Therefore, the unexpected 18 m GOC difference could be caused only by a subtle lateral nonequilibrium.

It should be noticed that the fitted asphaltene average molar mass (680 to 711) g·mol^{-1}, molar volume (669 to 697) cm^3·mol^{-1}, and diameter (1.28 to 1.30) nm are consistent with the values from the Yen–Mullins model,[10] such as the molar mass of an asphaltene monomer being about 750 g·mol^{-1}. The obtained results show that the colored asphaltene-like components are molecularly dispersed in the oil columns in the Norway field. This is also consistent with the processes of generating condensate reservoirs mentioned previously (not tending to generate asphaltenes but resins).

Case 2: Asphaltene Nanoaggregates in Stable Black Oil. Betancourt et al.[1] reported that highly undersaturated black oil in a 200 m vertical column was analyzed by DFA and advanced laboratory analytical chemistry methods. The oil samples were taken from two wells with low and similar GOR of about 125 m^3·m^{-3}. This is highly undersaturated black oil whose critical point and bubble point are far away from formation conditions. The asphaltene content in STO was analyzed by a standard *n*-heptane precipitation method. This case was also used to test the methodology proposed in this work. Similar to the Tahiti field,[51] the compositional and property gradients are small according to both the laboratory measurements and the EOS model. The fluids are highly undersaturated and rather incompressible; therefore, the hydrostatic head pressure in the reservoir does little to impact a compositional variation. Instead of the absolute pressure, it is the relative pressure difference in the 200 m vertical column of oil that plays an important role in generating gradients. It is impossible to conclude whether or not the oil column is connected in terms of the traditional compositional gradient method. Again, coupling the asphaltene gradient analysis with the other advanced chemical analyses could give a conclusion.

The delumped compositions (dotted curve) are compared with the laboratory measurements (open triangles) in Figure 6.
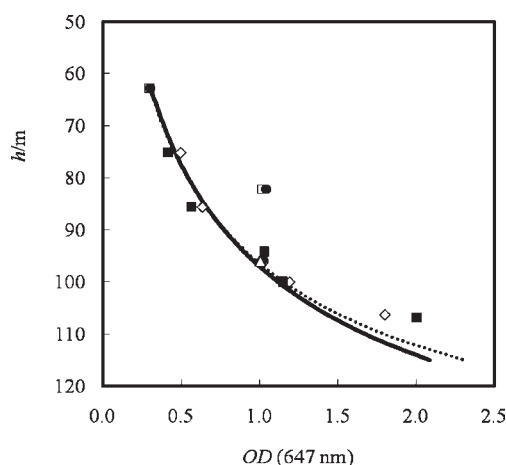
The fluid properties are matched by tuning the EOS model in the way mentioned previously. It is also presumed that asphaltenes are dispersed in the oil as asphaltene nanoaggregates. The three-parameter Γ-distribution function mentioned above was used to describe the molar mass distribution of asphaltene nanoaggregates at the reference point. The average molar mass was treated as an adjustable parameter by fitting the DFA-measured coloration gradient coloration data. The adjusted average molar mass values vary from (2886 to 3085) g·mol^{-1} in the 200 m depth interval from the top to bottom. Figure 11 shows coloration variations with relative depth. The coloration analysis shows that the sands in the oil column are connected and the black oils are in equilibrium. The two sands were indicated to be in pressure communication, a necessary but insufficient condition to establish flow communication on production time scales. The two black oils have similar low GORs, which is consistent with their being in equilibrium. Furthermore, the reservoir sand properties are consistent with the contained fluids being in equilibrium. The primary reservoir sand has a permeability of about $1 \cdot 10^{-12}$ m^2, which favors convective mixing (much faster than diffusive mixing). These conditions are very similar to those in the Tahiti reservoir,[51] which also appeared to be in equilibrium. The other advanced chemical analyses gave the same conclusion as described by Betancourt et al.[1]

Case 3: Coexisting Asphaltene Nanoaggregates and Clusters of Asphaltene Nanoaggregates in Black Oil with Asphaltenes Destabilized. In stable black oil, asphaltenes are dispersed as nanoaggregates, whereas in (movable) heavy oil, asphaltenes are stably suspended as clusters of asphaltene nanoaggregates.[10−12] If asphaltenes are destabilized in black oil, some nanoaggregates can form clusters, and thus nanoaggregates and clusters coexist in unstable black oil. Furthermore, at certain
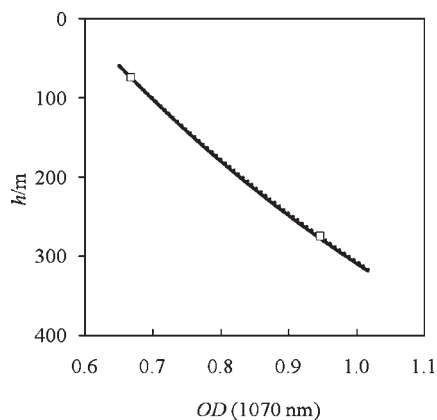
Figure 11. OD variations with relative depth h for case 2. The equilibrium nanoaggregate asphaltene profiling indicates that the reservoir is connected. The results are confirmed by the advanced chemical analysis (2-D GC) as shown in ref 1. □, measurements by LFA; —, calculation by the asphaltene-grading model with an average asphaltene molar mass of 2900 g·mol^{-1} at the reference depth; ···, calculation by the asphaltene-grading model with an average asphaltene molar mass of 2900 g·mol^{-1} at the reference depth and C_1 and C_{6+} composition (weight percent) deviations by 0.5 and 3, respectively.

points in the oil column, like the bottom, instability can be severe, yielding flocculation formation and forming clusters that deposit in the reservoir and may then form tar mats. When the system reaches equilibrium, nanoaggregates and clusters coexist in the black oil.

In particular, if asphaltene gradient with depth is very large in a black oil column, the diameter of common asphaltene nanoaggregates (≈ 2 nm) cannot be applicable to model the asphaltene (color) gradient. This behavior implies that (1) there exists not only the common asphaltene nanoaggregates with ≈ 2 nm in diameter but also asphaltene clusters that are much bigger in diameter than the common asphaltene nanoaggregates suspended in the oil columns; (2) large density and viscosity gradients are expected; (3) the oil may have a flow assurance problem (e.g., asphaltene onset pressure is equal to formation pressure, bitumens are found in formation cores); and (4) there might be an allochthonous tar mat (as opposed to autochthonous tar mats from biodegradation).

In this case study, the black oil has a GOR of ≈ 150 m^3·m^{-3}. The delumped compositions (dashed curve) are compared with the laboratory measurements (solid circles) in Figure 6 as well. The oil column has some GOR gradient and density gradient with depth. A fraction of asphaltenes is destabilized by the late stage gas charging. A huge color gradient was found: ≈ 10 times in about 80 m depth. The continuous pressure gradient data show that the oil zone is in pressure communication, which is a necessary but insufficient condition to establish flow connectivity. Figure 12 depicts an asphaltene (color) gradient in the destabilized black oil column.

The dotted curve is calculated by the Flory−Huggins model with clusters of asphaltene nanoaggregates (about 4 nm in diameter). The average molar masses change from (20 000 to 30 000) g·mol^{-1} within about 80 m depth interval. The assumption of only forming asphaltene clusters significantly overestimates the asphaltene gradient. On the other hand, the dashed curve is computed by the Flory−Huggins model with asphaltene nanoaggregates only (about 2 nm in diameter), which is similar to that in the black oil mentioned above. Obviously, the assumption of only
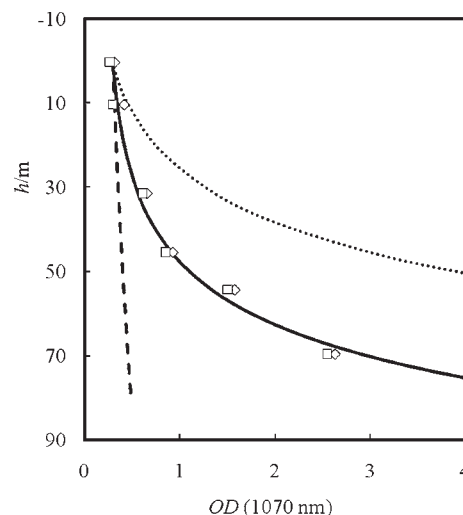

Figure 12. A huge OD (asphaltene) gradient in a destabilized black oil column. The asphaltene gradient is consistent with an equilibrium distribution of 80 % nanoaggregates with ≈ 2 nm in diameter + 20 % clusters with ≈ 4 nm in diameter. The continuous distribution implies formation connectivity, which is consistent with the corresponding vertical interference testing. ◇, measurements by LFA; □, measurements by IFA (in situ fluid analyzer); ---, calculation by the model with $z_1 = 1.0$ and $d_1 \approx 2$ nm; ···, calculation by the model with $z_1 = 0.0$ and $d_2 \approx 4$ nm; —, calculation by the model with $z_1 = 0.8$, $d_1 \approx 2$ nm and $d_2 \approx 4$ nm.

forming asphaltene nanoaggregates considerably underestimates the asphaltene gradient. The field data are in good agreement with an equilibrium distribution of 80 % asphaltene nanoaggregates + 20 % clusters. The equilibrium asphaltene distribution indicates that the oil zone is connected, which is consistent with the vertical interference testing and continuous pressure gradient (in spite of a necessary condition). The clusters are formed from a fraction of asphaltene nanoaggregates because the late stage gas charging (which is corroborated by a geochemistry analysis of volatile components) lowers the oil solvation power (solubility parameters) in the oil column and thus causes asphaltene destabilization. The analysis was confirmed by the field evidence: (1) the asphaltene onset pressure was equal to the formation pressure, and (2) bitumens were found in the core.

To compare variations of asphaltene molar mass distributions in the oil columns from the top to bottom sands, the normalized probability density functions are illustrated in Figure 13 for the three cases. Figure 14 depicts variations of the average asphaltene spherical diameters with depth. It can be seen that variations of asphaltene molar mass distributions and average asphaltene sizes with depth for asphaltene molecules and nanoaggregates are small. However, the variations of the asphaltene molar mass distributions and average asphaltene sizes with depth for asphaltene clusters are a bit large. More high molar mass components are present at the bottom sand than at the top sand. This is expected because unstable asphaltenes were deposited and bitumens were found in the core at the bottom of the oil reservoir.

Sensitivity Analysis. The optical measurements of relative asphaltene content (color) have exceedingly small uncertainties, and the optical measurements are very accurate. These uncertainties in the optical measurements of relative asphaltene content are at least an order of magnitude better than standard laboratory separation measurements.[53,54] This is one of the most robust measurements in DFA.
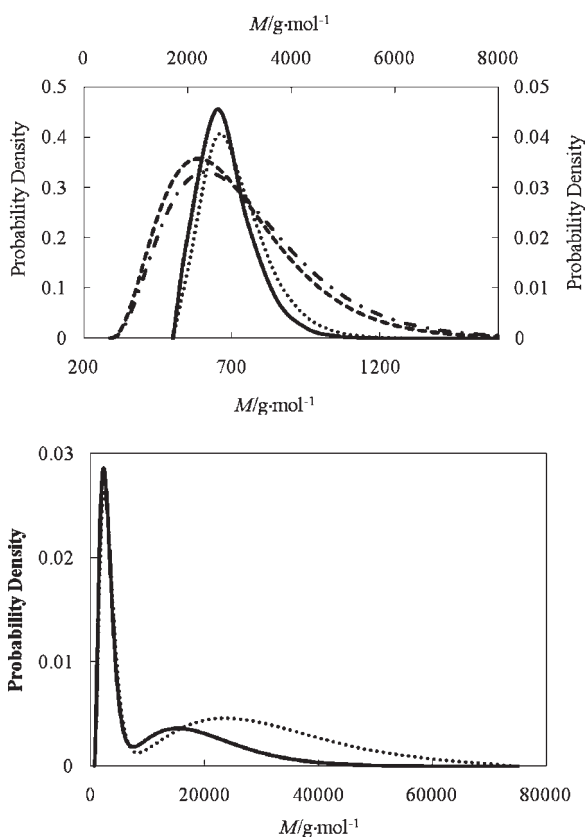
Figure 13. Distribution functions of asphaltene molar mass M. (a) Probability density vs M for cases 1 and 2 from the top to bottom sands. —, case 1 (top); ···, case 1 (bottom); ---, case 2 (top); -··-, case 2 (bottom). Asphaltene molar mass distributions vary slightly with depth. (b) Probability density vs M for case 3 from the top to bottom sands. —, case 3 (top); ···, case 3 (bottom); Asphaltene molar mass distributions vary slightly with depth for asphaltene nanoaggregates, while they considerably change for clusters.

Two key parameters (compositions of methane and hexane +) in DFA measurements are chosen to conduct sensitivity analysis, which are the most important variables in fluid property calculations. Thus, the input compositions of methane and hexane + in mass fraction are deviated by 0.5 % and 3 %, respectively. The EOS model is tuned to match live fluid density and then used to estimate compositional and property gradients with depth. The asphaltene grading model is used to calculate the asphaltene gradient along with the estimated fluid property gradients such as molar volume and molar mass. The color (asphaltene) gradient analysis results are also given in Figures 10 and 11 (dotted curves) for cases 1 and 2, respectively. The uncertainties of DFA measurements may cause some changes in the fluid compositional and property gradients for near critical and high GOR fluids, whereas there are slight changes for highly undersaturated black oil. However, the uncertainties of DFA measurements have a slight impact on asphaltene gradient analysis. Therefore, they do not influence any conclusions about reservoir connectivity analysis.

It can be seen from the presented color analysis that advanced asphaltene science provides a framework for understanding the molecular and/or colloidal dispersion of heavy ends in crude oil. Moreover, the DFA technology provides a measurement of GOR (compositions) and oil coloration in situ in oil wells, thereby
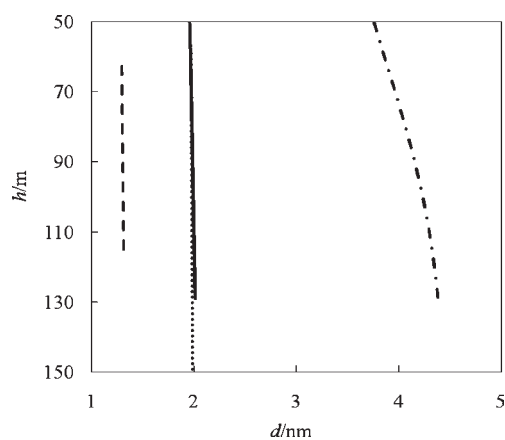

Figure 14. Variations of average asphaltene spherical diameters d with relative depth h for three cases. Asphaltene sizes slightly increase with depth for asphaltene molecules and nanoaggregates, while a more obvious increase is seen for asphaltene clusters. ---, asphaltene molecules with $d \approx 1.3$ nm in case 1; ····, asphaltene nanoaggregates with $d \approx 2$ nm in case 2; —, asphaltene nanoaggregates with $d \approx 2$ nm in case 3; -··-, clusters of asphaltene nanoaggregates with $d \approx 4$ nm in case 3.

obtaining the relative heavy-end concentration. The combination of the advanced asphaltene science, models, and DFA provides the means to evaluate connectivity and other complexities in reservoirs.

■ CONCLUSIONS

A new methodology was developed here to combine recent advances in asphaltene science with the DFA technology to address the biggest concerns today with reservoirs. In particular, this powerful combination of advanced asphaltene science, models, and DFA technology has been applied successfully to indicate reservoir connectivity. This novel approach was proved to work here and behooves future applications.

A new bimodal molar mass distribution function and a thermodynamic approach of EOS + solubility models were developed to calculate variations of asphaltenes with depth in reservoir fluid columns. The Peng–Robinson EOS with the Peneloux volume translation was first used to calculate compositional gradient of reservoir fluids for bulk reservoir fluids. Then the properties of the bulk oils with depth were estimated by the EOS for subsequent asphaltene (color) gradient analysis. The asphaltenes were then divided into three to five pseudocomponents (subfractions) by the Gaussian quadrature method and the proposed bimodal distribution function. The Flory–Huggins regular solution model for multicomponents was applied to compute asphaltenes profiling in reservoir columns. A few field case studies were used to validate the developed approach. The obtained results are consistent with advanced asphaltene science and show that the colored asphaltene-like components (resins) are molecularly dispersed in the oil columns (condensate reservoir), the asphaltenes are dispersed as nanoaggregates in the stable black oil reservoir, and the asphaltenes are dispersed/suspended as nanoaggregates and clusters in the unstable black oil reservoir. The asphaltene gradients that are consistent with an equilibrium distribution imply reservoir connectivity.

■ APPENDIX: BASIC TERMS USED IN THE OIL AND GAS INDUSTRY

GOR and API Gravity. When oil at downhole conditions is brought (flashed) to surface conditions, it is usual for some

Table 1. Classification of Oil and Gas[52]

oil type[a]	GOR $m^3 \cdot m^{-3}$	API gravity	color of stock-tank oil
heavy oil	< 20	< 25	black
black oil	20 to 356	25 to 40	very dark colored to black
volatile oil	356 to 588	> 40	colored, usually brown
gas condensate	588 to 890	50 to 60	lightly colored
wet gas	> 890	> 50	clear
dry gas	∞	no liquid	no liquid

[a] There are no definite boundaries between these classifications, and usage may vary depending on locations. GOR and API gravity are also dependent on separator conditions.

dissolved gas to come out of solution. The gas/oil ratio (GOR) is the ratio of the volume of gas that comes out of solution (flashed gas), to the volume of oil (stock-tank oil or flashed oil) at standard conditions (T = 288.7 K and p = 0.1 MPa). The specific gravity (SG) of stock-tank oil (STO) is defined as STO density in $g \cdot cm^{-3}$ divided by water density (1 $g \cdot cm^{-3}$) at standard conditions, which can be converted to API gravity according to

$$\text{API gravity} = \frac{141.5}{\text{SG}} - 131.5$$

Reservoir Fluids. Reservoir fluids are multicomponent mixtures, consisting primarily of hydrocarbons. They can be divided into three main classes: (1) defined components like methane, ethane, propane, and so forth; (2) single carbon number fractions like C_7, C_8, and so forth, and each fraction is still a mixture; and (3) plus fractions like C_{30+} (C_{30} and heavier components).[19] The flashed gas at surface conditions consists primarily of light ends of hydrocarbons, whereas the stock-tank oil can be separated into saturates, aromatics, resins, and asphaltenes (SARA) in laboratories.

Reservoir Fluid Classification. The classification of oil and gas is given in Table 1.

■ AUTHOR INFORMATION

Corresponding Author
*E-mail: yzuo@slb.com.

■ REFERENCES

(1) Betancourt, S. S.; Ventura, G. T.; Pomerantz, A. E.; Viloria, O.; Dubost, F. X.; Zuo, J.; Monson, G.; Bustamante, D.; Purcell, J. M.; Nelson, R. K.; Rodgers, R. P.; Reddy, C. M.; Marshall, A. G.; Mullins, O. C. Nanoaggregates of Asphaltenes in a Reservoir Crude Oil and Reservoir Connectivity. *Energy Fuels* **2009**, 23, 1178–1188.

(2) Dong, C.; Elshahawi, H.; Mullins, O. C.; Hows, M.; Venkataramanan, L.; McKinney, D.; Flannery, M.; Hashem, M. *Improved Interpretation of Reservoir Architecture and Fluid Contacts through the Integration of Downhole Fluid Analysis with Geochemical and Mud Gas Analyses*, Paper SPE 109683; SPE APOGCE, Jakarta, Indonesia, Oct 30—Nov 1, 2007.

(3) Dong, C.; O'Keefe, M.; Elshahawi, H.; Hashem, M.; Williams, S.; Stensland, D.; Hegeman, P.; Vasques, R.; Terabayashi, T.; Mullins, O. C.; Donzier, E. *New Downhole Fluid Analyzer Tool for Improved Reservoir Characterization*, Paper SPE 108566; SPE Offshore Europe Conference, Aberdeen, Scotland, U.K., Sept 4—7, 2007.

(4) Dubost, F. X.; Carnegie, A. J.; Mullins, O. C.; O'Keefe, M.; Betancourt, S. S.; Zuo, J. Y.; Eriksen, K. O. *Integration of In-Situ Fluid Measurements for Pressure Gradients Calculations*, Paper SPE 108494;

(5) Elshahawi, H.; Hashem, M. N.; Mullins, O. C.; Fujisawa, G. *The Missing Link—Identification of Reservoir Compartmentalization by Downhole Fluid Analysis*, Paper SPE 94709; SPE Annual Technical Conference and Exhibition, Houston, Texas, Oct 9—12, 2005.

(6) Gisolf, A.; Dubost, F. X.; Zuo, J.; Williams, S.; Kristoffersen, J.; Achourov, V.; Bisarah, A.; Mullins, O. C. *Real Time Integration of Reservoir Modeling and Formation Testing*, Paper SPE 121275; EUR-OPEC/EAGE Annual Conference and Exhibition, Amsterdam, June 8—11, 2009.

(7) Mullins, O. C.; Fujisawa, G.; Hashem, M. N.; Elshahawi, H. *Coarse and Ultra-Fine Scale Compartmentalization by Downhole Fluid Analysis Coupled*, Paper SPE IPTC 10034; ITPC, Doha, Qatar, Nov 21—23, 2005.

(8) Mullins, O. C.; Betancourt, S. S.; Cribbs, M. E.; Creek, J. L.; Dubost, F. X.; Andrews, A. B.; Venkataramanan, L. *Asphaltene Gravitational Gradient in a Deepwater Reservoir as Determined by Downhole Fluid Analysis*, Paper SPE 106375; SPE International Symposium on Oilfield Chemistry, Houston, TX, Feb 28—Mar 2, 2007.

(9) Mullins, O. C.; Sheu, E. Y.; Hammami, A.; Marshall, A. G., Eds. *Asphaltenes, Heavy Oils and Petroleomics*; Springer: New York, New York, 2007.

(10) Mullins, O. C. The Modified Yen Model. *Energy Fuels* **2010**, 24, 2179–2207.

(11) Mullins, O. C.; Zuo, J. Y.; Freed, D. E.; Elshahawi, H. *Downhole Fluid Analysis Coupled with Asphaltene Nano-science for Reservoir Evaluation*; Rio Oil & Gas Conference, Rio de Janeiro, Sept 13—16, 2010.

(12) Zuo, J. Y.; Mullins, O. C.; Freed, D.; Zhang, D. *DFA Profiling of Oil Columns Using Asphaltene Gradient*, Paper SPE #133656; 2010 SPE Annual Technical Conference and Exhibition, Florence, Italy, Sept 19—22, 2010.

(13) Zuo, J. Y.; Freed, D. E.; Mullins, O. C.; Zhang, D.; Gisolf, A. *Interpretation of DFA Color Gradients in Oil Columns Using the Flory-Huggins Solubility Model*, Paper SPE130305; CPS/SPE International Oil & Gas Conference and Exhibition, Beijing, China, June 8—10, 2010.

(14) Mullins, O. C.; Freed, D. E.; Zuo, J.; Elshahawi, H. *The Impact of Reservoir Fluid Compositional Variation and its Origin on Flow Assurance Evaluation*, Paper OTC20464; 2010 Offshore Technology Conference, Houston, TX, May 3—6, 2010.

(15) Mullins, O. C.; Zuo, J.; Freed, D. E.; Elshahawi, H.; Cribbs, M. E.; Mishra, V. K.; Gisolf, A. *Downhole Fluid Analysis Coupled with Novel Asphaltene Science for Reservoir Evaluation*; 51st Annual International SPWLA Conference, Perth, Australia, June 19—23, 2010.

(16) Whitson, C. H. Characterizing Hydrocarbon Plus Fractions. *Soc. Pet. Eng. J.* **1983**, 23, 683–694.

(17) Zuo, J. Y.; Zhang, D. *Plus Fraction Characterization and PVT Data Regression for Reservoir Fluids near Critical Conditions*, Paper SPE 64520; SPE Asia Pacific Oil and Gas Conference and Exhibition, Brisbane, Australia, Oct 16—18, 2000.

(18) Zuo, J. Y.; Zhang, D.; Dubost, F.; Dong, C.; Mullins, O. C.; O'Keefe, M.; Betancourt, S. S. *EOS-Based Downhole Fluid Characterization*, Paper SPE 114702; SPE Asia Pacific Oil & Gas Conference and Exhibition, Perth, Australia, Oct 20—22, 2008; accepted for publication in *SPE J.* in press, 2010.

(19) Pedersen, K. S.; Christensen, P. L. *Phase Behavior of Petroleum Reservoir Fluids*; CRC Press, Taylor & Francis Group: Boca Raton, FL, 2007.

(20) Firoozabadi, A. *Thermodynamics of Hydrocarbon Reservoir*; McGraw-Hill: New York, NY, 1999.

(21) Michelsen, M. L.; Mollerup, J. M. *Thermodynamic Models: Fundamentals & Computational Aspects*; Tie-Line Publications: Holte, Denmark, 2004.

(22) Ahmed, T. *Equations of State and PVT Analysis: Applications for Improved Reservoir Modeling*; Gulf Publishing Company: Houston, TX, 2007.

International Oil Conference and Exhibition, Veracruz, Mexico, June 27—30, 2007.

(23) Høier, L.; Whitson, C. H. Compositional Grading—Theory and Practice. *SPE Reservoir Eval. Eng.* 2001, *4*, 525–535.

(24) Montel, F.; Bickert, J.; Caillet, G.; Le Goff, C. *Modeling the Effect of External Gas Flux on Reservoir Fluid Description*, Paper SPE 77383; SPE Annual TCE, San Antonio, TX, Sept 29–Oct 2, 2002.

(25) Montel, F.; Bickert, J.; Hy-Billiot, J.; Royer, M. *Pressure and Compositional Gradients in Reservoirs*, Paper SPE 85668; SPE International Technical Conference and Exhibition, Abuja, Nigeria, Aug 4–6, 2003.

(26) Montel, F.; Bickert, J.; Lagisquet, A.; Galliero, G. Initial State of Petroleum Reservoirs: A Comprehensive Approach. *J. Petrol. Sci. Eng.* 2007, *58*, 391–402.

(27) Pedersen, K. S.; Lindeloff, N. *Simulations of Compositional Gradients in Hydrocarbon Reservoirs under the Influence of a Temperature Gradient*, Paper SPE 84364; SPE Annual Technical Conference and Exhibition, Denver, CO, Oct 5–8, 2003.

(28) Zuo, J. Y.; Mullins, O. C.; Dong, C.; Zhang, D.; O'Keefe, M.; Dubost, F; Betancourt, S. S.; Gao, J. *Integration of Fluid Log Predictions and Downhole Fluid Analysis*, Paper SPE 122562; SPE Asia Pacific Oil and Gas Conference and Exhibition, Jakarta, Indonesia, Aug 4–6, 2009.

(29) Zuo, J. Y.; Mullins, O. C.; Dong, C.; Betancourt, S. S.; Dubost, F. X.; O'Keeffe, M.; Zhang, D. *Investigation of Formation Connectivity Using Asphaltene Gradient Log Predictions Coupled with Downhole Fluid Analysis*, Paper SPE 124264; SPE Annual Technical Conference and Exhibition, New Orleans, LA, Oct 4–7, 2009.

(30) Zuo, J. Y.; Mullins, O. C.; Dong, C.; Zhang, D. Modeling of Asphaltene Grading in Oil Reservoirs. *Nat. Res.* 2010, *1*, 19–27.

(31) Vargas, F. M.; Gonzalez, D. L.; Hirasaki, G. J.; Chapman, W. G. Modeling Asphaltene Phase Behavior in Crude Oil Systems Using the Perturbed Chain Form of the Statistical Associating Fluid Theory (PC-SAFT) Equation of State. *Energy Fuels* 2009, *23*, 1140–1146.

(32) Gonzalez, D. L.; Hirasaki, G. J.; Creek, J.; Chapman, W. G. Modeling of Asphaltene Precipitation Due to Changes in Composition Using the Perturbed Chain Statistical Associating Fluid Theory Equation of State. *Energy Fuels* 2005, *21*, 1231–1242.

(33) Gonzalez, D. L.; Ting, P. D.; Hirasaki, G. J.; Chapman, W. G. Prediction of Asphaltene Instability under Gas Injection with the PC-SAFT Equation of State. *Energy Fuels* 2007, *19*, 1230–1234.

(34) Gonzalez, D. L.; Vargas, F. M.; Hirasaki, G. J.; Chapman, W. G. Modeling Study of CO_2-Induced Asphaltene Precipitation. *Energy Fuels* 2008, *22*, 757–762.

(35) Akbarzadeh, K.; Dhillon, A.; Svrcek, W. Y.; Yarranton, H. W. Methodology for the Characterization and Modeling of Asphaltene Precipitation from Heavy Oils Diluted with n-Alkanes. *Energy Fuels* 2004, *18*, 1434–1441.

(36) Alboudwarej, H.; Akbarzadeh, K.; Beck, J.; Svrcek, W. Y.; Yarranton, H. W. Regular Solution Model for Asphaltene Precipitation from Bitumens and Solvents. *AIChE J.* 2003, *49*, 2948–2956.

(37) Tharanivasan, A. K.; Svrcek, W. Y.; Yarranton, H. W.; Taylor, S. D.; Merino-Garcia, D.; Rahimi, P. Measurement and Modeling of Asphaltene Precipitation from Crude Oil Blends. *Energy Fuels* 2009, *23*, 3971–3980.

(38) Wang, J. X.; Buckley, J. S. A Two-Component Solubility Model of the Onset of Asphaltene Flocculation in Crude Oils. *Energy Fuels* 2001, *15*, 1004–1012.

(39) Mohammadi, A. H.; Richon, D. A Monodisperse Thermodynamic Model for Estimating Asphaltene Precipitation. *AIChE J.* 2007, *53*, 2940–2947.

(40) Hirschberg, A. Role of Asphaltenes in Compositional Grading of a Reservoir's Fluid Column. *J. Petrol. Technol.* 1988, *40*, 89–94.

(41) Freed, D. E.; Mullins, O. C.; Zuo, J. Y. Theoretical Treatment of Asphaltenes in the Presence of GOR Gradients. *Energy Fuels* 2010, *24*, 3942–3949.

(42) Prausnitz, J. M.; Lichtenthaler, R. N.; de Azevedo, E. G. *Molecular Thermodynamics of Fluid-Phase Equilibrium*; Prentice Hall: Upper Saddle River, NJ, 1999.

(43) Andreatta, G.; Bostrom, N.; Mullins, O. C. High-Q Ultrasonic Determination of the Critical Nanoaggregate Concentration of Asphaltenes and the Critical Micelle Concentration of Standard Surfactants. *Langmuir* 2005, *21*, 2728–2736.

(44) Zeng, H.; Song, Y. Q.; Johnson, D. L.; Mullins, O. C. Critical Nanoaggregate Concentration of Asphaltenes by Direct-Current (DC) Electrical Conductivity. *Energy Fuels* 2009, *23*, 1201–1208.

(45) Whitson, C. H.; Anderson, T. F.; Soreide, I. Application of the Gamma Distribution Model to Molecular Weight and Boiling Point Data for Petroleum Fractions. *Chem. Eng. Commun.* 1990, *96*, 259–278.

(46) Whitson, C. H.; Anderson, T. F.; Soreide, I. C_{7+} Characterization of Related Equilibrium Fluids Using the Gamma Distribution. In *C7+ Fraction Characterization*; Chorn, L. G., Mansoori, G. A., Eds.; Taylor & Francis Inc.: New York, NY, 1989.

(47) Peng, D.-Y.; Robinson, D. B. A New Two-Constant Equation of State. *Ind. Eng. Chem. Fundam.* 1976, *15*, 59–64.

(48) Peng, D.-Y.; Robinson, D. B. *The Characterization of the Heptanes and Heavier Fractions for the PGA Peng-Robinson Programs*, GPA Research Report RR-28; 1978.

(49) Peneloux, A.; Rauzy, E.; Freze, R. A Consistent Correction for Redlich-Kwong-Soave Volumes. *Fluid Phase Equilib.* 1982, *8*, 7–23.

(50) Zuo, J. Y.; Mullins, O. C.; Freed, D.; Zhang, D. A Simple Relation between Densities and Solubility Parameters for Live Reservoir Fluids. *J. Chem. Eng. Data* 2010, *55*, 2964–2969.

(51) Betancourt, S. S.; Dubost, F. X.; Mullins, O. C.; Cribbs, M. E.; Creek, J. L.; Mathews, S. G. *Predicting Downhole Fluid Analysis Logs to Investigate Reservoir Connectivity*, Paper SPE IPTC 11488; IPTC, Dubai, UAE, Dec 4–6, 2007.

(52) Mullins, O. C. *The Physical of Reservoir Fluids: Discovery through Downhole Fluid Analysis*; Schlumberger: Sugar Land, Texas, USA, 2008.

(53) Ruiz-Morales, Y.; Wu, X.; Mullins, O. C. Electronic Absorption Edge of Crude Oils and Asphaltenes Analyzed by Molecular Orbital Calculations with Optical Spectroscopy. *Energy Fuels* 2007, *21*, 944–952.

(54) Ruiz-Morales, Y. Molecular Orbital Calculations and Optical Transitions of PAHs and Asphaltenes. In *Asphaltenes, Heavy Oils and Petroleomics*; Mullins, O. C., Sheu, E. Y., Hammami, A., Marshall, A. G., Eds.; Springer: New York, NY, 2007; Chapter 4, pp 95–137.